

Nonparametric Estimation of Means on Hilbert Manifolds and Extrinsic Analysis of Mean Shapes of Contours

Leif Ellingson[‡], Vic Patrangenaru[†], and Frits Ruymgaart[‡]
[†]Florida State University and [‡]Texas Tech University

February 11, 2013

Abstract

Motivated by the problem of nonparametric inference in high level digital image analysis, we introduce a general extrinsic approach for data analysis on Hilbert manifolds with a focus on means of probability distributions on such sample spaces. To perform inference on these means, we appeal to the concept of neighborhood hypotheses from functional data analysis and derive a one-sample test. We then consider analysis of shapes of contours lying in the plane. By embedding the corresponding sample space of such shapes, which is a Hilbert manifold, into a space of Hilbert-Schmidt operators, we can define extrinsic mean shapes of planar contours and their sample analogues. We apply the general methods to this problem while considering the computational restrictions faced when utilizing digital imaging data. Comparisons of computational cost are provided to another method for analyzing shapes of contours.

Keywords: data analysis on Hilbert manifolds, extrinsic means, nonparametric bootstrap, planar contours, digital image analysis, automated randomized landmark selection, statistical shape analysis

1 Introduction

It is the purpose of this paper to introduce general methodology for data analysis on infinite dimensional Hilbert manifolds. Nonparametric procedures for inference on the population mean are included, focusing on an extrinsic approach. Theoretical results for both estimation and testing hypotheses are derived. Dette and Munk (1998) [40] rekindled the interest in neighborhood hypotheses by showing that they are appropriate and useful in a nonparametric functional context. Since “in practice” one cannot expect an infinite dimensional object to be exactly equal to a prescribed hypothesized object, the neighborhood hypothesis will be employed too in this paper.

*Research supported by National Science Foundation Grant DMS-0805977

†Research supported by National Science Foundation Grants DMS-0805977, DMS-1106935 and the National Security Agency Grant MSP-H98230-08-1-0058

Just as in finite dimensions, the general theory could be applied to a variety of special manifolds. However, here we will restrict ourselves to the important case of projective spaces that will be embedded in the Hilbert-Schmidt operators, which is useful in the analysis of shapes of infinite dimensional configurations lying in the plane. Necessary computational considerations are considered for the implementation of the methodology and the computational cost turns out to compare favorably with that of other procedures used in shape analysis.

Let us now turn to a brief discussion of the existing literature that is most relevant for the present paper. To the best of our knowledge, the combination of the theory for functional data in infinite dimensional linear spaces with the geometry for infinite dimensional manifolds for the purpose of nonparameteric analysis is new. There are, however, some procedures that seem to lack the underlying asymptotic theory needed for a nonparametric analysis. These will be reviewed along with some pertinent theoretical results for functional data, and some relevant existing methods for finite dimensional manifolds.

A number of statistical methodologies have been developed for the analysis of data lying on Hilbert spaces for the purpose of studying functional data. Some multivariate methods, such as PCA, have useful extensions in functional data analysis (Loève [33]). For dense functional data, the asymptotics of the resulting eigenvalues and eigenvectors were studied by Dauxois et. al. (1982) [10]. Even for sparse functional data, these methods have been proved useful (see Hall et. al. (2006)[17], Müller et. al.(2006)[39]) and have multiple applications. There are, nevertheless, techniques defined for multivariate analysis that often fail to be directly generalizable to infinite-dimensional data, especially when such data is nonlinear. New methodologies have been developed to account for these high dimensional problems, with many of these presented in a standard text by Ramsay and Silverman (2005) and given by references therein. For high dimensional inference on Hilbert spaces, Munk and Dette (1998) [40] utilized the concept of neighborhood hypotheses for performing tests on nonparametric regression models. Following from this approach, Munk *et al.* (2008) [41] developed one-sample and multi-sample tests for population means.

However these methods do not account for estimation of means on infinitely dimensional curved spaces, such as Hilbert manifolds. In order to properly analyze such data, these methods must be further generalized and modified. A key example in which such data arises is in the statistical analysis of direct similarity shapes of planar contours, which can be viewed as outlines of 2D objects in an image.

Unlike functional data analysis, which started from dense functional data and was extended to sparse functional data, the study of shapes in the plane originated with D. G. Kendall (1984) [23], which showed that the space Σ_2^k of direct similarity shapes of nontrivial planar finite configurations of k points is a complex projective space $\mathbb{C}P^{k-2}$. However, definitions of location and variability parameters for probability distributions were considered much later. While the full Procrustes estimate of a mean shape was defined by Kent (1992), a nonparametric definition of a mean shape was first introduced by Ziezold (1994) [54] based upon the notion of Fréchet population mean (Fréchet (1948) [12], Ziezold (1977) [55]). This approach was followed by Ziezold (1998) [53], Le and Kume (2000) [32], Kume and Le (2000 [28], 2003 [27]), Le (2001) [30], Bhattacharya and Patrangnearu (2003) [8], and Huckemann and Ziezold (2006) [18].

While a majority of these methods have defined means in terms of Riemannian distances, as initially suggested by Patrangenaru (1998) [42], a Veronese-Whitney (VW) extrinsic mean similarity shape was also introduced by Patrangenaru (op.cit.), in terms of the VW embedding of $\mathbb{C}P^{k-2}$ into the space $S(k-1, \mathbb{C})$ of selfadjoint $(k-1) \times (k-1)$ matrices. The asymptotic distribution of this extrinsic sample mean shape and the resulting bootstrap distribution are given in Bhattacharya and Patrangenaru (2005) [5], Bandulasiri et. al (2009) [4] and Amaral et al. (2010) [1].

Motivated by the pioneering work of Zahn and Roskies (1972) and by other applications in object recognition from digital images, Grenander (1993) [14] considered shapes as points on some infinite dimensional space. A manifold model for direct similarity shapes of planar closed curves, first suggested by Azencott (1994) [2], was pursued in Azencott et. al. (1996)[3], and detailed by Younes (1998 [49], 1999 [50]). This idea gained ground at the turn of the millennium, with more researchers studying shapes of planar closed curves (eg. Sebastian et. al. (2003) [45]).

Klassen et al. (2004) [26], Michor and Mumford (2004) [34] and Younes et al. (2008) [51] follow the methods of Small (1996) [46] and Kendall by defining a Riemannian structure on a shape manifold. Klassen et al. (op. cit) compute an intrinsic sample mean shape, which is a Fréchet sample mean for the chosen Riemannian distance. The related papers Mio and Srivastava (2004) [36], Mio et al. (2007) [38], Srivastava et al. (2005) [48], Mio et al. (2005) [37], Kaziska and Srivastava (2007) [21], and Joshi et al. (2007) [20] compute an intrinsic sample mean similarity shape of closed curves modulo reparameterizations, for a Riemannian metric of their preference, out of infinitely many Riemannian metrics available. To compute these types of means, those papers use iterative gradient search algorithms, as closed-form solutions for the means do not exist.

However, these approaches only consider computational aspects without addressing fundamental definitions of populations of shapes, population means and population covariance operators, thus making no distinction between a population parameter and its sample estimators. As such, the idea of statistical inference is absent from these papers.

This paper is organized as follows. In Section 2, we introduce methodology for data analysis on Hilbert manifolds, including a definition for the extrinsic mean (set) of a random object on an embedded Hilbert manifold and introduce an inference procedure for a neighborhood hypothesis for an extrinsic mean. In Section 3, we define the space of direct similarity shapes of planar contours. Section 4 is dedicated to the derivation of the asymptotic distribution of the extrinsic sample mean contour shape. Due to the infinite-dimensionality, the sample mean cannot be properly studentized, so in Section 5, we instead apply the neighborhood hypothesis test to this problem.

The remainder of the paper concerns application of the methodology to digital imaging data. In section 6 we address the representation, approximation, and correspondence problems faced when working with such data in practice. In Section 7, we present examples of the neighborhood hypothesis test using contours extracted from a database of silhouettes from digital images, collected by Ben Kimia [25]. In Section 8, we use nonpivotal nonparametric bootstrapping (see Efron (1979) [11], Hall (1992) [16]) to form confidence regions for the extrinsic mean shape for examples from the same database and compare computational speed of our method to that of Joshi et.

al. (2007) [20]. The paper ends with a discussion suggesting an extension of other methodologies from functional data or for data on finite dimensional manifolds to data analysis on Hilbert manifolds. An extension of the shape analysis methods to more complicated, infinite dimensional features captured in digital images, such as edge maps obtained from gray-level images, is also suggested.

2 Inference for means on Hilbert manifolds

In this section we assume that \mathbf{H} is a *separable, infinite dimensional Hilbert space* over the reals. Any such space is isometric with l_2 , the space of sequences $x = (x_n)_{n \in \mathbb{N}}$ of reals for which the series $\sum_{n=0}^{\infty} x_n^2$ is convergent, with the scalar product $\langle x, y \rangle = \sum_{n=0}^{\infty} x_n y_n$. A Hilbert space with the norm $\|v\| = \sqrt{\langle v, v \rangle}$, induced by the scalar product, becomes a Banach space. Differentiability can be defined with respect to this norm.

DEFINITION 2.1. A function f defined on an open set U of a Hilbert space \mathbf{H} is Fréchet differentiable at a point $x \in U$, if there is a linear operator $T : \mathbf{H} \rightarrow \mathbf{H}$, such that if we set

$$(1) \quad \omega_x(h) = f(x+h) - f(x) - T(h),$$

then

$$(2) \quad \lim_{h \rightarrow 0} \frac{\|\omega_x(h)\|}{\|h\|} = 0.$$

Since T in Definition 2.1 is unique, it is called the differential of f at x and is also denoted by $d_x f$.

DEFINITION 2.2. A chart on a separable metric space (\mathcal{M}, ρ) is a one to one homeomorphism $\varphi : U \rightarrow \varphi(U)$ defined on an open subset U of \mathcal{M} to a Hilbert space \mathbf{H} . A Hilbert manifold is a separable metric space \mathcal{M} , that admits an open covering by domain of charts, such that the transition maps $\varphi_V \circ \varphi_U^{-1} : \varphi_U(U \cap V) \rightarrow \varphi_V(U \cap V)$ are differentiable.

Example 1. The projective space $P(\mathbf{H})$ of a Hilbert space \mathbf{H} , the space of all one dimensional linear subspaces of \mathbf{H} , has a natural structure of Hilbert manifold modelled over \mathbf{H} . Define the distance between two vector lines as their angle, and, given a line $\mathbb{L} \subset \mathbf{H}$, a neighborhood $U_{\mathbb{L}}$ of \mathbb{L} can be mapped via a homeomorphism $\varphi_{\mathbb{L}}$ onto an open neighborhood of the orthocomplement \mathbb{L}^{\perp} by using the decomposition $\mathbf{H} = \mathbb{L} \oplus \mathbb{L}^{\perp}$. Then for two perpendicular lines \mathbb{L}_1 and \mathbb{L}_2 , it is easy to show that the transition maps $\varphi_{\mathbb{L}_1} \circ \varphi_{\mathbb{L}_2}^{-1}$ are differentiable as maps between open subsets in \mathbb{L}_1^{\perp} , respectively in \mathbb{L}_2^{\perp} . A countable orthobasis of \mathbf{H} and the lines $\mathbb{L}_n, n \in \mathbb{N}$ generated by the vectors in this orthobasis is used to cover $P(\mathbf{H})$ with the open sets $U_{\mathbb{L}_n}, n \in \mathbb{N}$. Finally, use the fact that for any line $\mathbb{L}, \mathbb{L}^{\perp}$ and \mathbf{H} are isometric as Hilbert spaces. The line \mathbb{L} spanned by a nonzero vector $\gamma \in \mathbf{H}$ is usually denoted $[\gamma]$ when regarded as a projective point on $P(\mathbf{H})$ and will be denoted as such henceforth.

Similarly, one may consider complex Hilbert manifolds, modeled on Hilbert spaces over \mathbb{C} . A vector space over \mathbb{C} can be regarded as a vector space over the reals, by restricting the scalars to \mathbb{R} ; therefore any complex Hilbert manifold automatically inherits a structure of real Hilbert manifold.

2.1 Extrinsic analysis of means on Hilbert manifolds

For Hilbert spaces that do not have a linear structure, standard methods for data analysis on Hilbert spaces cannot directly be applied. To account for this nonlinearity, one may instead perform extrinsic analysis by embedding this manifold in a Hilbert space.

DEFINITION 2.3. An embedding of a Hilbert manifold \mathcal{M} in a Hilbert space \mathbb{H} is a one-to-one differentiable function $j : \mathcal{M} \rightarrow \mathbb{H}$, such that for each $x \in \mathcal{M}$, the differential $d_x j$ is one to one, and the range $j(\mathcal{M})$ is a closed subset of \mathbb{H} and the topology of \mathcal{M} is induced via j by the topology of \mathbb{H} .

Example 2. We embed $P(\mathbf{H})$ in $\mathcal{L}_{HS} = \mathbf{H} \otimes \mathbf{H}$, the space of Hilbert-Schmidt operators of \mathbf{H} into itself, via the Veronese-Whitney (VW) embedding j given by

$$(3) \quad j([\gamma]) = \frac{1}{\|\gamma\|^2} \gamma \otimes \gamma.$$

If $\|\gamma\| = 1$, this definition can be reformulated as

$$(4) \quad j([\gamma]) = \gamma \otimes \gamma.$$

The range of this embedding is the submanifold \mathcal{M}_1 of rank one Hilbert-Schmidt operators of \mathbf{H} .

To define a location parameter for probability distributions on a Hilbert manifold, the concept of extrinsic means from Bhattacharya and Patrangenaru (2003, 2005)) is extended below to the infinite dimensional case.

DEFINITION 2.4. If $j : \mathcal{M} \rightarrow \mathbb{H}$ is an embedding of a Hilbert manifold in a Hilbert space, the chord distance ρ on \mathcal{M} is given by $\rho(x, y) = \|j(x) - j(y)\|$, and given a random object X on \mathcal{M} , the associated Fréchet function is

$$(5) \quad \mathcal{F}_j(x) = E(\|j(X) - j(x)\|^2).$$

The set of all minimizers of \mathcal{F}_j is called the extrinsic mean set of X . If the extrinsic mean set has one element only, that element is called the extrinsic mean and is labeled $\mu_{E,j}$ or simply μ_E .

PROPOSITION 2.1. Consider a random object X on \mathcal{M} that has an extrinsic mean set. Then (i) $j(X)$ has a mean vector μ and (ii) the extrinsic mean set is the set of all points $x \in \mathcal{M}$, such that $j(x)$ is at minimum distance from μ . (iii) In particular, μ_E exists if there is a unique point on $j(\mathbf{M})$ at minimum distance from μ , the projection $P_j(\mu)$ of μ on $j(\mathbf{M})$, and in this case $\mu_E = j^{-1}(P_j(\mu))$.

Proof. Let $Y = j(X)$. Note that the Hilbert space \mathbb{H} is complete as a metric space, therefore $\inf_{y \in \mathbb{H}} E(\|Y - y\|^2) = \min_{y \in \mathbb{H}} E(\|Y - y\|^2) \leq \min_{y \in j(\mathcal{M})} E(\|Y - y\|^2)$, and from our assumption, it follows that $\inf_{y \in \mathbb{H}} E(\|Y - y\|^2) = \min_{y \in \mathbb{H}} E(\|Y - y\|^2)$ is finite, which proves (i). To prove (ii), assume for ν is a point in the extrinsic mean set, and x is an arbitrary point on $\in \mathcal{M}$. From $E(\|j(\nu) - Y\|^2) \leq E(\|j(x) - Y\|^2)$ and, since $j(\nu) - \mu$ and $j(x) - \mu$ are constant vectors, it follows that

$$(6) \quad \|j(\nu) - \mu\|^2 \leq \|j(x) - \mu\|^2 + 2E(\langle j(x) - j(\nu), \mu - Y \rangle).$$

It is obvious that the expected value on the extreme righthand side of equation (6) is zero. We now consider a property that is critical for having a well-defined, unique extrinsic mean.

DEFINITION 2.5. A random object X on a Hilbert manifold \mathcal{M} embedded in a Hilbert space is j -nonfocal if there is a unique point p on $j(\mathcal{M})$ at minimum distance from $E(j(X))$.

Example 3. The unit sphere $S(\mathbb{H}) = \{x \in \mathbb{H}, \|x\| = 1\}$ is a Hilbert manifold embedded in \mathbb{H} via the inclusion map $j : S(\mathbb{H}) \rightarrow \mathbb{H}, j(x) = x$. A random object X on $S(\mathbb{H})$ of mean μ is j -nonfocal, if $\mu \neq 0$.

Using this property, one may give an explicit formula for the extrinsic mean for a random object on $P(\mathbf{H})$ with respect to the VW embedding, which we will call VW mean.

PROPOSITION 2.2. Assume $X = [\Gamma]$ is a random object in $P(\mathbf{H})$. Then the VW mean of X exists if and only if $E(\frac{1}{\|\Gamma\|^2} \Gamma \otimes \Gamma)$ has a simple largest eigenvalue, in which case, the distribution is j -nonfocal. In this case the VW mean is $\mu_E = [\gamma]$, where γ is an eigenvector for this eigenvalue.

Proof. We select an arbitrary point $[\gamma] \in P(\mathbf{H}), \|\gamma\| = 1$. The spectral decomposition of $\Lambda = E(\frac{1}{\|\Gamma\|^2} \Gamma)$ is $\Lambda = \sum_{k=1}^{\infty} \delta_k^2 E_k, \delta_1 \geq \delta_2 \geq \dots$ where for all $k \geq 1, E_k = e_k \otimes e_k, \|e_k\| = 1$, therefore if $\gamma = \sum_{k=1}^{\infty} x_k e_k, \sum_{k=1}^{\infty} x_k^2 < \infty$, then $\|j(\gamma) - \mu\|^2 = \|\gamma \otimes \gamma\|^2 + \sum_{k=1}^{\infty} \delta_k^2 - 2 \langle \Lambda, \gamma \otimes \gamma \rangle$. To minimize this distance it suffices to maximize the projection of the unit vector $\gamma \otimes \gamma$ on Λ . If $\delta_1 = \delta_2$ there are the vectors $\gamma_1 = e_1$ and $\gamma_2 = e_2$ are both maximizing this projection, therefore there is a unique point $j([\gamma])$ at minimum distance from Λ if and only if $\delta_1 > \delta_2$. A definition of a covariance parameter is also needed in order to define asymptotics and perform inference on an extrinsic mean. The following result is a straightforward extension of the corresponding finite dimensional result in Bhattacharya and Patrangenaru (2005). The tangential component $\tan(v)$ of $v \in \mathbb{H}$ w.r.t. the orthobasis $e_a(P_j(\mu)) \in T_{P_j(\mu)}j(\mathcal{M}), a = 1, 2, \dots, \infty$ is given by

$$(7) \quad \tan(v) = \sum_{a=1}^{\infty} (e_a(P_j(\mu)) \cdot v) e_a(P_j(\mu)).$$

Then given the j -nonfocal random object X , extrinsic mean μ_E , and covariance operator of $\tilde{\Sigma} = cov(j(X))$, if $f_a(\mu_E) = d_{\mu_E}^{-1}(e_a(P_j(\mu))), \forall a = 1, 2, \dots$, then X has

extrinsic covariance operator represented w.r.t. the basis $f_1(\mu_E), \dots$ by the infinite matrix $\Sigma_{j,E}$:

$$(8) \quad \left[\sum d_\mu P_j(e_b) \cdot e_a(P_j(\mu)) \right]_{a=1,\dots} \tilde{\Sigma} \left[\sum d_\mu P_j(e_b) \cdot e_a(P_j(\mu)) \right]_{a=1,\dots}^T \Sigma_{j,E} =$$

With extrinsic parameters of location and covariance now defined, the asymptotic distribution of the extrinsic mean can be shown as in the final dimensional case (see Bhat-tacharya and Patrangenaru (2005)[9]):

PROPOSITION 2.3. Assume X_1, \dots, X_n are i.i.d. random objects (r.o.'s) from a j -nonfocal distribution on a Hilbert manifold \mathcal{M} , for a given embedding $j : \mathcal{M} \rightarrow \mathbf{H}$ in a Hilbert space \mathbf{H} with extrinsic mean μ_E and extrinsic covariance operator Σ . Then, with probability one, for n large enough, the extrinsic sample mean $\bar{X}_{n,E}$ is well defined. If we decompose $j(\bar{X}_{n,E}) - j(\mu_E)$ with respect to the scalar product into a tangential component in $T_{j(\mu_E)}j(\mathcal{M})$ and a normal component $N_{j(\mu_E)}j(\mathcal{M})$, then

$$(9) \quad \sqrt{n}(\tan(j(\bar{X}_{n,E}) - j(\mu_E))) \rightarrow_d \mathcal{G},$$

where \mathcal{G} has a Gaussian distribution in $T_{j(\mu_E)}j(\mathcal{M})$ with extrinsic covariance operator $\Sigma_{j,E}$.

2.2 A one-sample test of the neighborhood hypothesis

Following from a neighborhood method in the context of regression by Munk and Dette (1998)[40], Munk et al. (2008)[41] developed tests for means of random objects on Hilbert spaces. We now adapt this methodology for tests for extrinsic means. First, however, we will need the following useful extension of Cramer's delta method. The proof is left to the reader.

THEOREM 2.1. For $a = 1, 2$ consider an embedding $j_a : \mathcal{M}_a \rightarrow \mathbf{H}_a$ of a Hilbert manifold \mathcal{M}_a in a Hilbert space \mathbf{H}_a . Assume X_1, \dots, X_n are i.i.d. r.o.'s from a j_1 -nonfocal distribution on \mathcal{M}_1 for a given embedding $j_1 : \mathcal{M}_1 \rightarrow \mathbf{H}_1$ in a Hilbert space \mathbf{H}_1 , with extrinsic mean μ_E and extrinsic covariance operator Σ . Let $\varphi : \mathcal{M}_1 \rightarrow \mathcal{M}_2$ be a differentiable function, such that $\varphi(X_1)$ is a j_2 -nonfocal r.o. on \mathcal{M}_2 . Then

$$(10) \quad \sqrt{n} \tan_{j_2(\varphi(\mu_E))}(j_2(\varphi(\bar{X}_{n,E})) - j_2(\varphi(\mu_E))) \rightarrow_d Y,$$

where $Y \sim \mathcal{N}(0, d_{\mu_E} \varphi^* \Sigma d_{\mu_E} \varphi)$. Here L^* is the adjoint operator of L .

We can now define the neighborhood hypothesis procedure for tests of extrinsic means. Assume Σ_j is the extrinsic covariance operator of a random object X on the Hilbert manifold \mathcal{M} , with respect to the embedding $j : \mathcal{M} \rightarrow \mathbb{H}$. Let \mathbf{M}_0 be a compact submanifold of \mathcal{M} . Let $\varphi_0 : \mathcal{M} \rightarrow \mathbb{R}$ be the function

$$(11) \quad \varphi_0(p) = \min_{p_0 \in \mathbf{M}_0} \|j(p) - j(p_0)\|^2,$$

and let $\mathbf{M}_0^\delta, \mathbf{B}_0^\delta$ be given respectively by

$$(12) \quad \begin{aligned} \mathbf{M}_0^\delta &= \{p \in \mathcal{M}, \varphi_0(p) \leq \delta^2\}, \\ \mathbf{B}_0^\delta &= \{p \in \mathcal{M}, \varphi_0(p) = \delta^2, \}. \end{aligned}$$

Since φ_0 is Fréchet differentiable and all small enough $\delta > 0$ are regular values of φ_0 , it follows that \mathbf{B}_0^δ is a Hilbert submanifold of codimension one in \mathcal{M} . Let ν_p be the normal space at a points $p \in \mathbf{B}_0^\delta$, orthocomplement of the tangent space to \mathbf{B}_0^δ at p . We define $\mathbf{B}_0^{\delta, X}$

$$(13) \quad \mathbf{B}_0^{\delta, X} = \{p \in \mathbf{B}_0, \Sigma_j|_{\nu_p} \text{ is positive definite}\}.$$

DEFINITION 2.6. The neighborhood test consists of testing the following two hypotheses:

$$(14) \quad \begin{aligned} H_0 &: \mu_E \in \mathbf{M}_0^\delta \cup \mathbf{B}_0^{\delta, X}, \\ H_A &: \mu_E \in (\mathbf{M}_0^\delta)^c \cap (\mathbf{B}_0^{\delta, X})^c. \end{aligned}$$

Munk et al. (2008) [41] show that, in general, the test statistic for these types of hypotheses has an asymptotically standard normal distribution for large sample sizes, in the case of random objects on Hilbert spaces. Here, we consider neighborhood hypothesis testing for the particular situation in which the submanifold \mathbf{M}_0 consists of a point m_0 on \mathcal{M} . We set $\varphi_0 = \varphi_{m_0}$, and since $T_{m_0}\{m_0\} = 0$ we will prove the following result.

THEOREM 2.2. If $M_0 = \{m_0\}$, the test statistic for the hypotheses specified in (14) has an asymptotically standard normal distribution and is given by:

$$(15) \quad T_n = \sqrt{n}\{\varphi_{m_0}(\hat{\mu}_E) - \delta^2\}/s_n,$$

where

$$(16) \quad s_n^2 = 4\langle \hat{\nu}, S_{E,n}\hat{\nu} \rangle$$

and

$$(17) \quad \begin{aligned} S_{E,n} &= \frac{1}{n} \sum_{i=1}^n (\tan_{\hat{\mu}} d_{j(X)_n} P_j(j(X_i) - \overline{j(X)_n})) \otimes \\ &\otimes (\tan_{\hat{\mu}} d_{j(X)_n} P_j(j(X_i) - \overline{j(X)_n})) \end{aligned}$$

is the extrinsic sample covariance operator for $\{X_i\}_{i=1}^n$, and

$$(18) \quad \hat{\nu} = (d_{\hat{\mu}_{E,n}} j)^{-1} \widehat{\tan}_{j(\hat{\mu}_{E,n})}(j(m_0) - j(\hat{\mu}_{E,n})).$$

Proof. The function φ_0 given in equation (11) defined on \mathcal{M} can be written as a composite function $\varphi_0 = \Phi_A \circ j$, where $\Phi_A(x) = \|x - A\|^2$ is differentiable on $\mathbb{H} \setminus \{A\}$, with the differential at x given by $d_x \Phi_A(y) = 2 \langle y, x - A \rangle$. Since $j(\mathcal{M})$

is a submanifold of \mathbb{H} , the restriction ϕ_A of $\Phi_A(x)$ to $j(\mathcal{M})$ is a differentiable function, with the differential

$$(19) \quad d_p \phi_A(y) = 2 \langle y, p - A \rangle, \forall y \in T_p j(\mathcal{M}).$$

Note that $\varphi_{m_0}(p) = \phi_{j(m_0)}(j(p))$, therefore, given that the differential $d_p j$ is a vector space isomorphism, we obtain

$$(20) \quad d_p \varphi_{m_0}(u) = 2 \langle d_p j(u), j(p) - j(m_0) \rangle, \forall u \in T_p \mathcal{M},$$

and in particular

$$(21) \quad d_{\mu_E} \varphi_{m_0}(u) = 2 \langle d_{\mu_E} j(u), j(\mu_E) - j(m_0) \rangle, \forall u \in T_{\mu_E} \mathcal{M},$$

that is

$$(22) \quad d_{\mu_E} \varphi_{m_0} = 2 d_{\mu_E} j \otimes \tan(j(\mu_E) - j(m_0)).$$

Since the null hypothesis (14) is accepted as long as $\varphi_{m_0}(\mu_E) < \delta^2$, we derive the asymptotic distribution of $\varphi_{m_0}(\hat{\mu}_E)$ under $\varphi_{m_0}(\mu_E) = \delta^2$. From Proposition 2.1, it follows that

$$(23) \quad \sqrt{n}(\varphi_{m_0}(\hat{\mu}_E) - \varphi_{m_0}(\mu_E)) \rightarrow_d Y,$$

where $Y \sim \mathcal{N}(0, (d_{\mu_E} \varphi_{m_0})^* \Sigma_E d_{\mu_E} \varphi_{m_0})$, we see that the random variable

$$(24) \quad Z_n = \frac{\sqrt{n}(\varphi_{m_0}(\hat{\mu}_E) - \varphi_{m_0}(\mu_E))}{\sqrt{(d_{\mu_E} \varphi_{m_0})^* \Sigma_E d_{\mu_E} \varphi_{m_0}}}$$

has asymptotically a standard normal distribution. From equation (22), if we set

$$(25) \quad \begin{aligned} \nu &= (d_{\mu_E} j)^{-1} \tan(j(\mu_E) - j(m_0)), \\ \sigma^2 &= 4 \langle \nu, \Sigma_E \nu \rangle, \end{aligned}$$

then

$$(26) \quad Z_n = \frac{\sqrt{n}(\varphi_{m_0}(\hat{\mu}_E) - \delta^2)}{\sigma}$$

Finally we notice that $\hat{\nu}$ in (18) is a consistent estimator of ν in (25), therefore s_n^2 in equation (16) is a consistent estimator of σ^2 in equation (25) and from Slutsky's theorem it follows that the test statistic T_n in equation (15) has asymptotically a $\mathcal{N}(0, 1)$ distribution.

3 Similarity shape space of planar contours

Features extracted from digital images are represented by planar subsets of unlabeled points. If these subsets are uncountable, the labels can be assigned in infinitely many ways. Here we will consider only contours, which are unlabeled boundaries of 2D

topological disks in the plane. To keep the data analysis stable, and to assign a *unique* labeling, we make the *generic* assumption that there is a unique point p_0 on such a contour at the maximum distance to its center of mass so that the label of any other point p on the contour is the counterclockwise travel time at constant speed from p_0 to p . As such, the total time needed to travel from p_0 to itself around the contour once is the length of the contour. Therefore we consider direct similarity shapes of nontrivial contours in the plane as described here. A contour $\tilde{\gamma}$ is then regarded as the range of a piecewise differentiable function, that is parameterized by arclength, i.e. $\gamma : [0, L] \rightarrow \mathbb{C}$, $\gamma(0) = \gamma(L)$ and is one-to-one on $[0, L)$. Recall that the length of a piecewise differentiable curve $\gamma : [a, b] \rightarrow \mathbb{R}^2$ is defined as follows:

$$(27) \quad l(\tilde{\gamma}) = \int_a^b \left\| \frac{d\gamma}{dt}(t) \right\| dt,$$

and its center of mass (mean of a uniform distribution on $\tilde{\gamma}$) is given by

$$(28) \quad z_{\tilde{\gamma}} = \frac{1}{L} \int_{\tilde{\gamma}} z ds.$$

The contour $\tilde{\gamma}$ is said to be regular if γ is a simple closed curve and there is a unique point $z_0 = \operatorname{argmax}_{z \in \tilde{\gamma}} \|z - z_{\tilde{\gamma}}\|$.

A direct similarity is a complex polynomial function in one variable of degree one. Two contours $\tilde{\gamma}_1, \tilde{\gamma}_2$ have the same direct similarity shape if there is a direct similarity $S : \mathbb{C} \rightarrow \mathbb{C}$, such that $S(\tilde{\gamma}_1) = \tilde{\gamma}_2$. The centered contour $\tilde{\gamma}_0 = \tilde{\gamma} - z_{\tilde{\gamma}} = \{z - z_{\tilde{\gamma}}, z \in \tilde{\gamma}\}$ has the same direct similarity shape as $\tilde{\gamma}$.

DEFINITION 3.1. Two regular contours $\tilde{\gamma}_1, \tilde{\gamma}_2$ have the same similarity shape if $\tilde{\gamma}_{2,0} = \lambda \tilde{\gamma}_{1,0}$, where λ is a nonzero complex number.

In order to construct the space of direct similarity shapes, we note the following.

REMARK 3.1. A function $\gamma : S^1 \rightarrow \mathbb{C}$ is *centered* if $\int_{S^1} \gamma(z) ds = 0$. We consider regular contours since the complex vector space spanned by centered functions γ yielding regular contours $\tilde{\gamma}$ is a pre-Hilbert space. Henceforth, we will be working with the closure of this space. This Hilbert space \mathbf{H} can and will be identified with the space of all measurable square integrable centered functions from S^1 to \mathbb{C} .

Let Σ_2^{reg} be the set of all direct similarity shapes of regular contours, which is the same as the space of all shapes of regular contours centered at zero.

REMARK 3.2. From Definition 3.1 and Remark 3.1, we associate a unique piecewise differentiable curve γ to a contour $\tilde{\gamma}$ by taking $\gamma(0) = z_0$, the point at the maximum distance to the center of C , and by parameterizing γ using arc length in the counter clockwise direction. Therefore Σ_2^{reg} is a dense and open subset of $P(\mathbf{H})$, the projective space corresponding to the Hilbert space \mathbf{H} . Henceforth, to simplify the notation, we will omit the symbol $\tilde{\cdot}$ in $\tilde{\gamma}$ and identify a regular contour with the associated closed curve, without confusion.

4 The Extrinsic Sample Mean Direct Similarity Shape and its Asymptotic Distribution

Note, from Example 2, that $P(\mathbf{H})$ is a Hilbert manifold which is VW-embedded in the Hilbert space \mathcal{L}_{HS} , and, from Proposition 2.3, the VW mean μ_E of a r.o. $X = [\Gamma]$ in $P(\mathbf{H})$, is $[e_1]$, where e_1 is the eigenvector corresponding to the largest eigenvalue of $\mu = E(\frac{1}{\|\Gamma\|^2}\Gamma \otimes \Gamma)$.

PROPOSITION 4.1. Given any VW-nonfocal probability measure Q on $P(\mathbf{H})$, then if $\gamma_1, \dots, \gamma_n$ is a random sample from Γ , then, for n large enough, the VW sample mean $\hat{\mu}_{E,n}$ is the projective point of the eigenvector corresponding to the largest eigenvalue of $\frac{1}{n} \sum_{i=1}^n \frac{1}{\|\gamma_i\|^2} \gamma_i \otimes \gamma_i$.

We can now derive the asymptotic distribution of $\hat{\mu}_{E,n}$ based upon the general formulation specified in Proposition 2.3. The asymptotic distribution of $\overline{j(X)}_n$ is as follows:

$$(29) \quad \sqrt{n}(\overline{j(X)}_n - \mu) \rightarrow_d \mathcal{G} \text{ as } n \rightarrow \infty,$$

where \mathcal{G} has a Gaussian distribution $N_{\mathcal{L}_{HS}}(0, \Sigma)$ on \mathcal{L}_{HS} a zero mean and covariance operator Σ . From Proposition 2.2, it follows that the projection $P_j : \mathcal{L}_{HS} \rightarrow j(P(\mathbf{H})) \subset \mathcal{L}_{HS}$ is given by

$$(30) \quad P_j(A) = \nu_A \otimes \nu_A,$$

where ν_A is the eigenvector of norm 1 corresponding to the largest eigenvalue of A , $P_j(\mu) = j(\mu_E)$, and $P_j(\overline{j(X)}_n) = j(\hat{\mu}_{E,n})$. Applying the delta method to (29) yields

$$(31) \quad \sqrt{n}(j(\hat{\mu}_{E,n}) - j(\mu_E)) \rightarrow_d N_{\mathcal{L}_{HS}}(0, d_\mu P_j \Sigma (d_\mu P_j)^T),$$

as $n \rightarrow \infty$, where $d_\mu P_j$ denotes the differential, as in Definition 2.1, of the projection P_j , evaluated at μ . It remains to find the expression for $d_\mu P_j$. To determine the formula for the differential, we must consider the equivariance of the embedding J . Because of this, we may assume without loss of generality that $\mu = \text{diag}\{\delta_a^2\}_{a=1,2,3,\dots}$. As defined previously, the largest eigenvalue of μ is a simple root of the characteristic polynomial, with e_1 as the corresponding complex eigenvector of norm 1, where $\mu_E = [e_1]$. An orthobasis for $T_{[e_1]}P(\mathbf{H})$ is formed by e_a, ie_a , for $a = 2, 3, \dots$, where e_a is the eigenvector over \mathbb{R} that corresponds to the a -th eigenvalue. For any γ which is orthogonal to e_1 w.r.t. the real scalar product, we define the path $\psi_\gamma(t) = [\cos(t)e_1 + \sin(t)\gamma]$. Then $T_{j([e_1])}j(P(\mathbf{H}))$ is generated by the vectors tangent to such paths at $t = 0$. Such vectors have the form $\gamma \otimes e_1 + e_1 \otimes \gamma$. In particular, since the eigenvectors of μ are orthogonal w.r.t. the complex scalar product, we may take $\gamma = e_a, a = 2, 3, \dots$, or $\gamma = ie_a, a = 2, 3, \dots$ to get an orthobasis for $T_{j([e_1])}j(P(\mathbf{H}))$. Normalizing these vectors to have unit lengths, we obtain the following orthonormal frame for $a = 2, 3, \dots$:

$$(32) \quad d_\mu j(e_a) = 2^{-1/2}(e_a \otimes e_1 + e_1 \otimes e_a),$$

$$(33) \quad d_\mu j(ie_a) = i2^{-1/2}(e_a \otimes e_1 + e_1 \otimes e_a),$$

As stated previously, since the map j is equivariant, we may assume that $\overline{j(X)}_n$ is a diagonal operator D , with the eigenvalues $\delta_1^2 > \delta_2^2 \geq \dots$. In this case,

$$(34) \quad d_{\mu_E} j(e_a) = 2^{-1/2} E_a^1 = F_a^1,$$

$$(35) \quad d_{\mu_E} j(i e_a) = i 2^{-1/2} E_a^1 = i F_a^1,$$

where E_a^b has all entries zero except those in the positions (a, b) and (b, a) that are all equal to 1. From these formulations and computations of the differential of P_j in the finite dimensional case in Bhattacharya and Patrangenaru (2005), it follows that $d_D P_j(E_a^b) = 0$, for all values $a \leq b$, except for $a = 1 < b$. In this case

$$(36) \quad d_D P_j(F_1^b) = \frac{1}{\delta_1^2 - \delta_b^2} F_1^b, \quad d_D P_j(i F_1^b) = \frac{1}{\delta_1^2 - \delta_b^2} i F_1^b.$$

Equation (36) implies that the differential of the projection P_j at μ is the operator Q_1 given by

$$(37) \quad Q_1 = \sum_{k=2}^{\infty} \frac{1}{\delta_1^2 - \delta_k^2} E_k,$$

where $\delta_1^2, \delta_2^2, \dots$ are the eigenvalues of $E(\frac{1}{\|\Gamma\|^2} \Gamma \otimes \Gamma)$ and E_1, E_2, \dots are the corresponding eigenprojections. Also, in this situation, \mathcal{G} is a normally distributed random element in \mathcal{L}_{HS} . This results in the tangential component of the difference between the j -images of the VW sample mean and of the VW mean having an asymptotic normal distribution, albeit with a degenerate covariance operator. From these computations, the asymptotic distribution of this difference can be expressed more explicitly in the following manner.

$$(38) \quad \sqrt{n}(\tan(j(\hat{\mu}_{E,n}) - j(\mu_E))) \xrightarrow{d} Q_1 \mathcal{G},$$

where $\tan(v)$ is the tangential component of $v \in j(P(\mathbf{H}))$ with respect to the basis $e_a(P_j(\mu)) \in T_{P_j(\mu)} j(P(\mathbf{H}))$, for $a = 2, 3, \dots$ and is expressed as

$$(39) \quad \tan(v) = (e_2(P_j(\mu))^T v, e_3(P_j(\mu))^T v, \dots)^T.$$

However, this result cannot be used directly because Q_1 , which is calculated using the eigenvalues of $E(\frac{1}{\|\Gamma\|^2} \Gamma \otimes \Gamma)$, and μ_E are unknown. This problem is solved by estimating μ_E by $\hat{\mu}_{E,n}$ and Q_1 in the following manner.

$$(40) \quad \hat{Q}_1 = \sum_{k=2}^{\infty} \frac{1}{\hat{\delta}_1^2 - \hat{\delta}_k^2} \hat{E}_k,$$

where $\hat{\delta}_1, \hat{\delta}_2, \dots$ are the eigenvalues of

$$(41) \quad \hat{\mu} = \frac{1}{n} \sum_{i=1}^n \frac{1}{\|\gamma_i\|^2} \gamma_i \otimes \gamma_i$$

and $\hat{E}_1, \hat{E}_2, \dots$ are the corresponding eigenprojections. Using this estimation, the asymptotic distribution is as follows:

$$(42) \quad \sqrt{n}(\widehat{\tan}(j(\hat{\mu}_{E,n}) - j(\mu_E))) \stackrel{d}{\approx} \hat{Q}_1 \mathcal{G},$$

where “ $\stackrel{d}{\approx}$ ” denotes approximate equality in distribution and $\widehat{\tan}$ is the tangential component relative to the tangent space of $j(P(\mathbf{H}))$ at $j(\hat{\mu}_{E,n})$ as in (39), where μ is replaced with $\hat{\mu}$ in equation (41). Applying this result to (31), we arrive at the following.

THEOREM 4.1. If $\Gamma_1, \dots, \Gamma_n$ are i.i.d.r.o.’s from a VW-nonfocal distribution Q on $P(\mathbf{H})$ with VW extrinsic sample mean $\hat{\mu}_{E,n}$, then

$$(43) \quad \sqrt{n}(j(\hat{\mu}_{E,n}) - j(\mu_E)) \stackrel{d}{\approx} d_{\hat{\mu}_n} P_j \mathcal{G} \text{ as } n \rightarrow \infty,$$

where $\hat{\mu}_n = \overline{j(X)}_n$ is a consistent estimator of μ .

REMARK 4.1. It must be noted that because of the infinite dimensionality of \mathcal{G} , in practice, a sample estimate for the covariance that is of full rank cannot be found. Because of this issue, this result cannot be properly studentized. Rather than using a regularization technique for the covariance that leads to complicated shape data computations, we will drastically reduce the dimensionality via the use of the neighborhood hypothesis methodology presented in Section 2.2. This type of approach showed its efficiency in projective shape analysis of planar curves in Munk et al. (2008).

5 The One-Sample Neighborhood Hypothesis Test for Mean Shape

Suppose that $j : P(\mathbf{H}) \rightarrow \mathcal{L}_{HS}$ is the VW embedding in (3) and $\delta > 0$ is a given positive number. Using the notation in Section 2, we now can apply Theorem 2.2 to random shapes of regular contours. Assume $x_r = [\gamma_r]$, $\|\gamma_r\| = 1$, $r = 1, \dots, n$ is a random sample from a VW-nonfocal probability measure Q . Then equation (43) shows that asymptotically the tangential component of the VW-sample mean around the VW-population mean has a complex multivariate normal distribution. Note that such a distribution has a Hermitian covariance matrix (see Goodman, 1963 [15]), therefore in this setting, the extrinsic covariance operator and its sample counterpart are infinite-dimensional Hermitian matrices. In particular, if we extend the CLT for VW-extrinsic sample mean Kendall shapes in Bhattacharya and Patrangenaru (2005), to the infinite dimensional case, the j -extrinsic sample covariance operator $S_{E,n}$, when regarded as an infinite Hermitian complex matrix has the following entries

$$(44) \quad S_{E,n,ab} = n^{-1}(\hat{\delta}_1^2 - \hat{\delta}_a^2)^{-1}(\hat{\delta}_1^2 - \hat{\delta}_b^2)^{-1} \sum_{r=1}^n \langle e_a, \gamma_r \rangle \langle e_b, \gamma_r \rangle^* | \langle e_1, \gamma_r \rangle |^2, a, b = 2, 3, \dots$$

with respect to the complex orthobasis e_2, e_3, e_4, \dots of unit eigenvectors in the tangent space $T_{\hat{\mu}_{E,n}}P(\mathbf{H})$. Recall that this orthobasis corresponds via the differential $d_{\hat{\mu}_{E,n}}$ with an orthobasis (over \mathbb{C}) in the tangent space $T_{j(\hat{\mu}_{E,n})}j(P(\mathbf{H}))$, therefore one can compute the components $\hat{\nu}^a$ of $\hat{\nu}$ from equation (18) with respect to e_2, e_3, e_4, \dots , and derive for s_n^2 in (16) the following expression

$$(45) \quad s_n^2 = 4 \sum_{a,b=2}^{\infty} S_{E,n,ab} \hat{\nu}^a \overline{\hat{\nu}^b},$$

where $S_{E,n,ab}$ given in equation (44) are regarded as entries of a Hermitian matrix. The test statistic T_n in equation (15) is defined on an infinite dimensional Hilbert manifold. In the next section we will explain how to accurately compute approximations of T_n based on finite dimensional polygonal approximations of the regular contours.

6 Approximation of Planar Contours

Ideally, the shapes of planar contours could be studied directly. However, when performing computations, it is necessary to approximate the contour by evaluating the function at only a finite number of times. If k such stopping times are selected, then the linear interpolation of the yielded stopping points is a k -gon z , for which each stopping time is a vertex. As with the contour, z is a one-to-one piecewise differentiable function that can be parametrized by arclength. Let L_k denote the length of the k -gon. For $j = 1, \dots, k$, let $z(t_j)$ denote the j th ordered vertex, where $t_j \in [0, L_k)$ and $z(t_1) = z(0) = z(L_k)$. It follows that, for $s \in (0, 1)$, the k -gon can be expressed as follows:

$$(46) \quad z(sL_k) = \begin{cases} (t_2 - sL_k)z(0) + sL_k z(t_2) & 0 < sL_k \leq t_2 \\ (t_j - sL_k)z(t_{j-1}) + (sL_k - t_{j-1})z(t_j) & t_{j-1} < sL_k \leq t_j \\ (L_k - sL_k)z(t_k) + (sL_k - t_k)z(0) & t_k < sL_k < L_k \end{cases}$$

for $j = 3, \dots, k$. As such, the space of direct similarity shapes of non-self-intersecting regular polygons is dense in the space of direct similarity shapes of regular contours. Therefore, the theory and methodology discussed in sections 3 through 5 hold for the shapes of these functions, as well. For the purposes of inference using the neighborhood hypothesis, then, it suffices to use the test statistic as derived previously. However, when considering these approximations, it is important to choose the stopping times appropriately so that the contour is well approximated by the polygon. Additionally, one must take correspondence across contours into consideration when working with a sample. We will first present an algorithm for choosing stopping times in such a way that the k -gon well represents the contour and converges to it accordingly. Following that, we will address considerations for working with samples.

6.1 Random Selection of Stopping Times

To obtain approximations, we propose to randomly select a large number k of stopping times t_j from the uniform distribution over $[0, L)$. By doing so, we insure, on

one hand, that we ultimately use a sufficiently large number of vertices so that the k -gon well represents the contour. On the other hand, we ensure the desired density of stopping points. In order to maintain the within sample matching for a sample of regular contours, we first find the point z_0 at the largest distance from the center of the contour and choose that as $z(0)$. We then randomly select $k - 1$ stopping times from the uniform distribution to form the k -gon, making sure to maintain the proper ordering, preventing the k -gon from self-intersecting. This is accomplished by sorting the selected stopping times in increasing order. It is important to choose an appropriate number of stopping times for the given data. The selected stopping points will be distributed fairly uniformly around the contour for large values of k , ensuring that the curve is accurately represented by the k -gon. However, choosing too many stopping times will needlessly increase the computational cost of performing calculations. This will be most noticeable when utilizing bootstrap techniques to compute confidence regions for the extrinsic mean shape. Choosing too few stopping times, though, while keeping computational cost down, can be extremely detrimental as the stopping points may not be sufficiently uniform to provide adequate coverage of the contour. This can significantly distort the k -gon, as shown in Fig.1. In this particular instance, the 200-gon of the dog includes no information about the lower jaw of the dog and little detail about one of the ears. The length of the contour L can be used to assist in determining

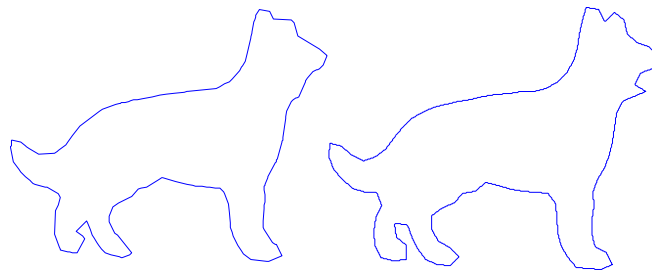


Figure 1: A 200-gon (left) and the associated contour (right) of a dog

an appropriate number of stopping points to be chosen. After selecting an initial set of

k stopping times as describe above, the length L_k of the k -gon is

$$(47) \quad L_k = \sum_{j=2}^{k+1} \|z(t_j) - z(t_{j-1})\|,$$

where $z(t_{k+1}) = z(0)$. An appropriate lower bound for the number of stopping points can be determined by randomly selecting times for various values of k . Compute L_k for each of these k -gons using (47) and compute the relative error compared to L . This should be repeated many times to obtain a mean relative error and standard deviation of the relative error for each value of k used. To determine an appropriate number of stopping points to use, compare the mean relative error to a desired threshold. Additionally, the distributions of the relative errors could also be examined. It should be noted, however, that since digital imaging data is discrete by nature, the contour will be represented by K pixels. As such, it is often necessary to replace L by L_K , the length of the closest approximation to the contour, which can be calculated similarly to L_k . When using this algorithm to select stopping points, it follows that the k -gon will converge to the contour. However, when selecting an additional stopping time $t_{j'}$, care must be taken to properly alter z in such a way that ensures that there is no self-intersection of the k -gon. To do so, simply reorder the stopping times in increasing order and apply the resulting permutation to the stopping points. It follows that, with probability 1, the length of the k -gon between successive stopping points will converge to 0 as the number of stopping times tends to infinity. This can be stated more formally as follows.

LEMMA 6.1. If stopping times s_1, s_2, \dots, s_k are selected from a uniform distribution over $[0, 1)$, then

$$L_{max} = \max_{j=2, k+1} \|z(s_j L_k) - z(s_{j-1} L_k)\| \xrightarrow{p} 0.$$

Proof.

$$\begin{aligned} P(L_{max} > \epsilon) &= P(\text{All } k \text{ stopping points are within the remaining } L_k - \epsilon) \\ &= P\left(\text{All } k \text{ stopping times are within the remaining } 1 - \frac{\epsilon}{L_k}\right) \end{aligned}$$

We can assume without loss of generality that the section of the k -gon for which the distance between successive stopping times is greater than ϵ^* is over the interval $(0, \epsilon)$. In addition, since the stopping times are independently chosen,

$$P(L_{max} > \epsilon) = \left(F(1) - F\left(\frac{\epsilon}{L_k}\right)\right)^k = \left(1 - \frac{\epsilon}{L_k}\right)^k$$

where F is the cdf for the uniform distribution over the interval $[0, 1)$. Taking the limit of this expression as $k \rightarrow \infty$ results in $L_{max} \xrightarrow{p} 0$ since

$$\lim_{k \rightarrow \infty} P(L_{max} > \epsilon) = \lim_{k \rightarrow \infty} \left(1 - \frac{\epsilon}{L_k}\right)^k = 0$$

□

It follows immediately that the center of mass of the k -gon converges to the center of mass of the contour. While the k -gon z converges to the contour γ , it is also of great interest to consider the convergence of $[z]$ to $[\gamma]$. Since z and γ are objects in the same space, the disparity in their shapes can be examined by considering the squared distance $\|j([z]) - j([\gamma])\|^2$ in \mathcal{L}_{HS} . However, for the purposes of computational comparisons, it is necessary to evaluate the functions at $m > k$ times using (46) and approximate the distance in $S(m, \mathbb{C})$, the space of self-adjoint $m \times m$ matrices. To illustrate, consider the contour considered in Figure 2. The digital representation

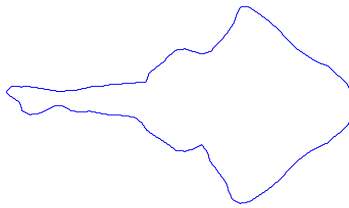


Figure 2: The digital image of the contour of a stingray.

of this contour consists of $K = 764$ pixels. Stopping times were selected using the above algorithm to form k -gons for $k = 3, \dots, 763$. Each k -gon was then evaluated at 764 times corresponding to the each of the pixels on the digital image of the contour. As such, squared distances between the k -gons and the contour were computed in $S(764, \mathbb{C})$. After this was repeated 50 times, the means and standard deviations of the squared distances were calculated for each value of k and are shown in Figure 3. The mean squared distance to the contour converges quickly, showing that the distance between $[z_k]$ and $[\gamma]$ only diminishes slightly for $k > 100$. Moreover, the variability introduced by selecting the stopping times randomly also rapidly approaches 0. As such, it is clear that $[\gamma]$ is well approximated using $k \ll K$. However, while the overall shape is well approximated, it is unclear from this alone how well the details of γ are approximated. As such, using the distance between shapes may not be the best indicator for determining a lower bound for k . For this purpose, it may be more helpful to consider $(L_K - L_k)/L_K$, the relative error in the approximation of the length, as described previously. For the contour in Figure 2, the relative error in length is shown in Figure 4. Here, while the variability approaches 0 quickly, the average relative error approaches 0 at a lower rate. As such, if it is desirable to keep the relative error below 0.05, for this example, no fewer than 300 stopping times should be selected.

6.2 Considerations for samples of contours

In addition to ensuring that each contour in a sample is well approximated, since each contour must be evaluated at m times for computations, it is necessary that each be eva-

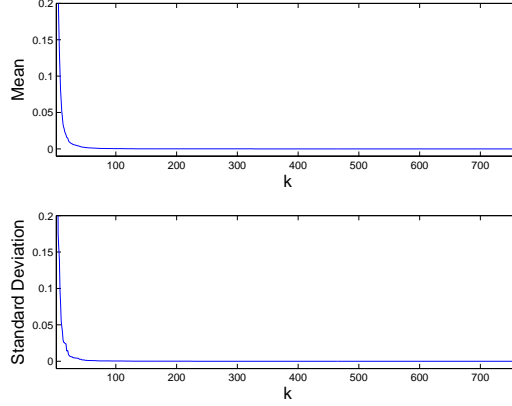


Figure 3: The mean and standard deviation of the squared distance of shapes of k -gons to the shape of the contour, as evaluated in $S(764, \mathbb{C})$.

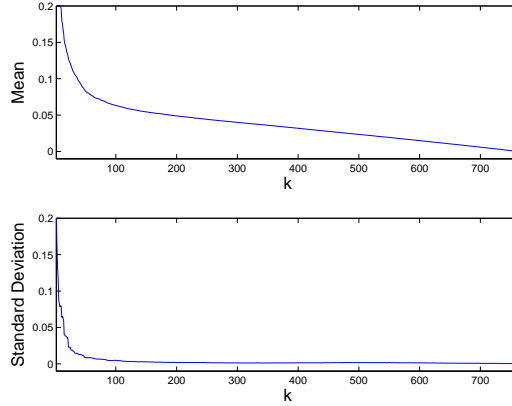


Figure 4: The mean and standard deviation of the relative error of the length of the k -gons.

luated at the same times to maintain correspondence across the n observations. In the ideal scenario, if each contour is well approximated by a k -gon, then select k stopping times $s_1, \dots, s_k \in [0, 1)$ using the algorithm as described above. For $j = 1, \dots, n$, the stopping points for z_j can then be obtained by evaluating γ_j at times $s_1 \cdot L^j, \dots, s_k \cdot L^j$, where L^j denotes the length of γ_j . Fig. 5 shows two examples of utilizing this procedure for samples of contours of hand gestures. Using the same stopping times for each observation, 6 stopping points are highlighted in red to illustrate the correspondence across the sample. Alternatively, if contour j requires k_j stopping points for adequate approximation, where $k_i \neq k_j$ for at least one pair i, j , then select stopping times for each contour. Let \mathcal{T}_j denote the set of stopping times that generate the k_j -gon z_j . In

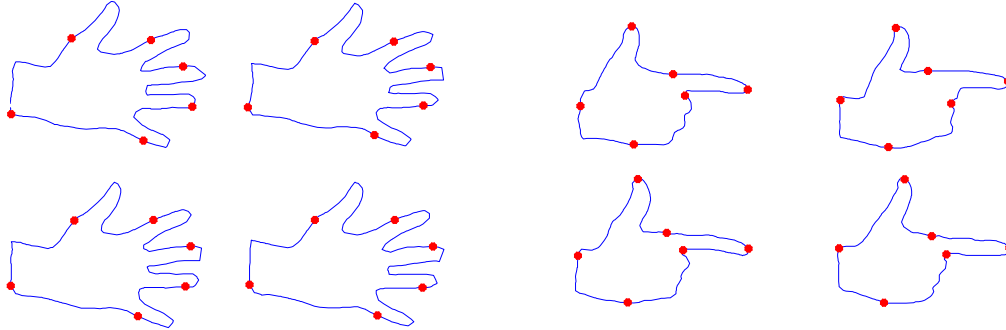


Figure 5: Correspondence of 6 stopping points for contours of hand gestures of (a) the number '5' and (b) the letter 'L'

order to maintain correspondence, evaluate z_j at the m times contained in $\cup_{i=1}^n \mathcal{T}_i$ for $j = 1, \dots, n$. This approach may also be utilized if each contour is approximated using k stopping points, but at different times. Finally, even if the conditions of either of the previous scenarios are met, it may be desired to consistently work within the same shape space when working with multiple samples, so it may be preferred to instead first consider approximating the contours and then approximating each at m subsequently chosen times, thus separating the issues of approximation and correspondence. However, for each of these scenarios, the selection of stopping points, evaluation of the k -gon at m times, and subsequent analysis can be either semi-automated or fully automated, allowing for efficient execution of the methodology.

6.3 Approximation of the sample mean shape

Whenever one is dealing with an object that is conceptually of infinite, or very high, dimension, a suitable dimension reduction must inevitably take place to enable computers to handle this object. Because this process is usually a projection from an infinite dimensional sample space of which the original object is an element, onto a finite dimensional subspace, we will for convenience refer to it as a “projection”. In the current situation, the infinite dimensional object is the average of projection operators $\hat{\mu}$ in equation (41), which is a positive element in the Hilbert space of Hilbert-Schmidt operators. Above, this object has been approximated by rather high-dimensional projection and then successively by projections of lower dimension, in order to arrive at an approximation of sufficiently low dimension that is still a good representative of the original object. What constitutes “good” here has not been established rigorously, but instead primarily on eye ball fitting, which may, in many cases, work rather well. A more sophisticated approach seems possible, however, and might be based on a method employed in the simulation of Brownian motion to determine a suitable number of points at which the values of the process should be simulated (Gaines, 2012 [13]). The objective in this special case was to ensure that the first few largest eigenvalues of the

covariance operator of the projection would approximate those of the original Brownian motion with prescribed accuracy. This could be achieved by using expansions for the eigenvalues of the projection in terms of those of the original process, known from perturbation theory. Since the statistic of main interest in the application considered in this paper is the largest eigenvalue of $\hat{\Gamma}$, a similar approach should, in principle, be appropriate in the present context. However, the problem of formally approximating infinite dimensional objects is a topic in its own right that is beyond the scope of the present paper, and that should, moreover, be considered in a more general context than presented by the situation at hand.

7 Application of the Neighborhood Hypothesis Test for Mean Shape

The test discussed in Section 5 could be performed for a variety of applications. The most likely applications involve having a known extrinsic mean shape determined from historical data. In such cases, the hypothesis test can be used to determine whether there is a significant deviation from the historical mean shape. An application in agriculture would be determining whether the use of a new fertilizer treatment results in the extrinsic mean shape of a crop significantly changing from the historical mean. Similarly, this test could be performed for quality control purposes to determine if there is a significant defect in the outline of an produced good. In practice, δ will be determined by the application and the decision for a test would be reached in the standard fashion. However, for the examples presented here, there is no natural choice for δ , so one can instead consider setting $Z = \xi_{1-\alpha}$ and solving for δ to show what decision would be reached for any value of δ . To do so, it is important to understand the role of δ . The size of the neighborhood around m_0 is completely determined by δ . As such, it follows that smaller values of δ result in smaller neighborhoods. In terms of H_0 , this places a greater restriction on M_δ and B_δ , requiring μ_E to have a smaller distance to m_0 . For the examples presented here, the contours are approximated using $k = 300$ stopping times, so the shape space is embedded into $S(300, \mathbb{C})$ to conduct analysis. In this environment, consider having two k -gons that are identical except for at one time. If this exceptional point for the second k -gon differs from the corresponding point in the first k -gon by a difference of 0.01 units, then the distance between the shapes inherited from $S(300, \mathbb{C})$ is approximately 0.0141. For the hypothesis test, if $\delta = 0.0141$, then the neighborhood around m_0 would consist of distances between shapes similar in scope to the situation described above. First, consider an example for which the one sample test for extrinsic mean shape is performed for sting ray contours. In this case, the sample extrinsic mean shape for a sample of contours of $n = 10$ sting rays is the shape shown on the left hand side in Fig. 6. After performing the calculations, it was determined that for an asymptotic level 0.05 test, the largest value of δ for which we would reject the null hypothesis is 0.0290. For perspective, this neighborhood has a radius roughly 2 times larger than the example with the nearly identical k -ads described above. This means that we would only reject the null hypothesis if we required the sample extrinsic mean to be nearly identical to the hypothesized mean. It should

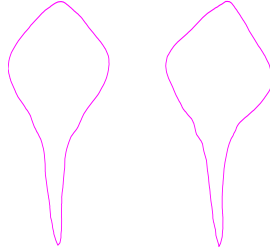


Figure 6: The extrinsic sample mean shape of a sample of 10 sting ray contours and, respectively, the hypothesized extrinsic mean shape

also be noted here that the sample size is small here, but that the conclusion agrees with intuition based upon a visual inspection of the contours. Now consider two examples involving contours of pears. In this first case, the sample consists of $n = 87$ pears. The sample extrinsic mean shape and hypothesized extrinsic mean shape are shown in Fig 7. It was determined that for an asymptotic level 0.05 test, the maximum value of δ

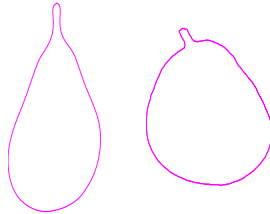


Figure 7: The extrinsic sample mean shape of a sample of 87 pear contours and, respectively, the hypothesized extrinsic mean shape

for which we would reject the null hypothesis is 1.2941. This value of δ is almost 92 times greater than the distance between the nearly identical k -ads. This suggests that even if we greatly relax the constraints for similarity, the null hypothesis would still be rejected. This again agrees with intuition. In this last example, consider another sample of contours of pears. In this scenario, we consider a sample of $n = 83$ pears. The sample extrinsic mean shape and hypothesized extrinsic mean shape are shown in Fig 8. After performing the calculations, we determined that for an asymptotic level 0.05 test, the largest value of δ for which we would reject the null hypothesis is 0.1969, meaning that our procedure does not reject the null hypothesis, unless δ is smaller than 0.1969. For perspective, this neighborhood has a radius nearly 14 times larger than

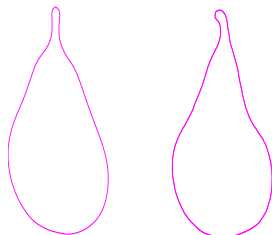


Figure 8: The extrinsic sample mean shape of a sample of 83 pear contours and, respectively, the hypothesized extrinsic mean shape

the example with the nearly identical k -ads described above. Unlike in the previous two examples it is unclear whether the null hypothesis should be rejected in this case without having a specific application in mind and, as such, this could be considered a borderline case.

8 Bootstrap Confidence Regions for Means of Shapes of Contours

Another method for performing inference, which we consider now, is through the use of nonparametric nonpivotal bootstrap. By repeatedly resampling from the available data and computing the distance between each resampled mean and the sample mean, we can obtain a confidence region for the extrinsic mean shape (for the sparse case, see Bandulasiri et al. (2008) [4] and Amaral et al (2010) [1]). The following examples of 95% nonparametric nonpivotal bootstrap confidence regions illustrate this approach using 400 resamples and serve to illustrate a methodology for visually understanding the confidence regions and their behavior. For each example, the sample is displayed on the left and the 95% confidence region is displayed on the right in blue with the extrinsic sample mean plotted in red. The first example, shown in Fig. 9, reveals that the confidence regions are wider in the portions of the shape in which there is more variability in the sample. Here, the bands are thicker in the regions corresponding to the tail and the top and bottom of the front section of the stingray, where the variability is the greatest. Secondly, samples with less variability result in narrower confidence regions. This can be seen by comparing Figs. 9 and 10. It is easy to see that there is less overall variability in the shapes of the contours of the wormfish than there is for the stingrays, which is reflected in the widths of the confidence regions. Furthermore, the effect of sample size on the confidence regions is clearly displayed in Fig. 11. As should be expected, the confidence region constructed using 88 observations is substantially thinner than that constructed using just 20 observations. In addition to being able to obtain sensible and intuitive results, the processing time needed to

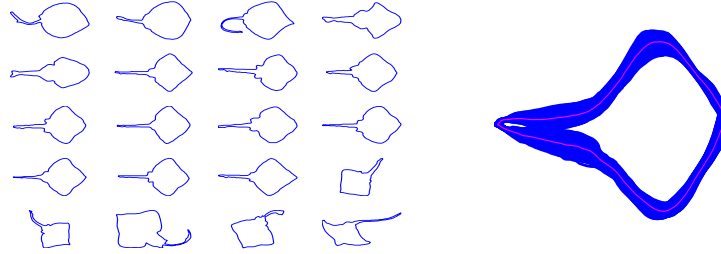


Figure 9: Bootstrap 95% confidence regions for the extrinsic mean shape of stingray contours using a sample of size 20.

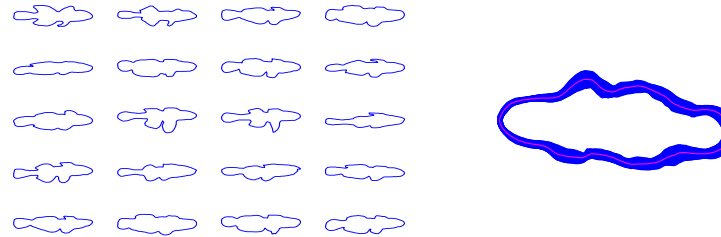


Figure 10: Bootstrap 95% confidence regions for the extrinsic mean shape of wormfish contours using a sample of size 20.

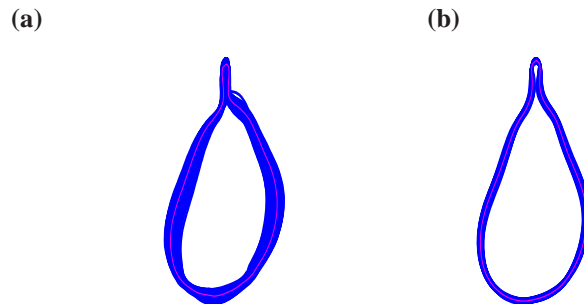


Figure 11: Bootstrap 95% confidence region for the extrinsic mean shape for the pears based on (a) 20 observations and (b) 88 observations.

compute bootstrap confidence regions for the VW extrinsic mean is small compared to doing the same using the elastic framework for the analyzing the shape of planar curves. The higher computational cost is due to a combination of the intrinsic analysis and the elastic representation. The calculation of an intrinsic mean requires the use of an iterative algorithm. The square-root elastic framework of Joshi et al. (2007) [20] adapts the algorithm of Klassen et al. (2004) for arc-length parametrized curves by in-

serting a reparametrization step at each iteration. This reparametrization step requires the use of either a dynamic programming algorithm or a gradient descent approach. These time-consuming steps are repeated a number of times during the calculation of the intrinsic mean, which, when obtaining a bootstrap confidence region, results in the computational cost being further compounded. As an example, this methodology was performed on a sample of hand gestures representing the letter “L” using the concepts of elastic shape representation, as described in Joshi *et al.* (2007) [20], and our methodology. The resulting confidence regions are given in Fig. 12. Using MATLAB on a machine running Windows XP on an Intel Core 2 Duo processor running at 2.33 GHz, these computations required 47.9 hours for the elastic method and only 47.5 seconds for ours. The difference in the size of the contours displayed in Fig.12 is due to the approaches using different methods for normalization. While we scale the complex vector denoting the coordinates for the contour at the sampled times to have a norm of 1, the square-root elastic framework scales curves to have unit length. While both methods perform well at producing estimates for mean shape and providing bootstrap confidence regions, our approach is far more computationally efficient. For a more detailed account of the advantages of extrinsic analysis of data on manifolds, especially for obtaining bootstrap confidence regions, see also Bhattacharya *et al.*(2012)[7].

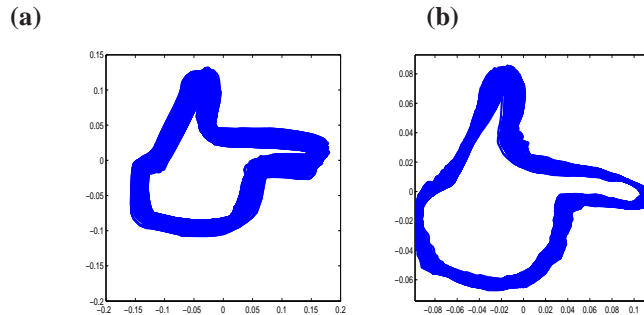


Figure 12: Bootstrap 95% confidence regions for (a) the intrinsic mean shape, as defined by Joshi *et al.* (2007), and (b) the extrinsic mean shape of the “l” hand gesture.

9 Discussion

In this paper, we have described how to address the neighborhood hypothesis for one population mean on a Hilbert manifold. This first paper on data analysis on a Hilbert manifold opens up a new area for data analysis of infinite dimensional objects that can not be represented on a Hilbert space. This is a rich domain for further study, with potential extensions and techniques coming from recent advances in statistics on finite dimensional manifolds and data analysis on infinite dimensional Hilbert spaces. Regarding applications in shape analysis, while our theory and computational methodology leads to the estimation of the extrinsic mean direct similarity shapes of planar contours, this approach could be extended further to any infinite configurations in the Euclidean plane, including 1-dimensional CW-complexes and planar domains, given

that the plane is separable. For example, one may consider shapes of edge maps obtained from gray-level images. In these cases, the problem of properly matching becomes much more difficult because, not only do points on a given edge from one image need to be matched to corresponding points on the corresponding edge in another image, but each edge in an image must be matched to the corresponding edge in another image, as well.

Additionally, we have only considered inference techniques for one-sample problems. While two-sample and multi-sample procedures may be more practical for many data analysis purposes, both the one-sample neighborhood hypothesis test and the non-pivotal nonparametric bootstrap confidence regions are useful nonparametric techniques for the estimation of the extrinsic mean shape for planar contours. In addition, they serve as an important first step towards the development and/or adapting of the desired two-sample and multi-sample procedures.

Furthermore, it should be noted that planar contour data carries with it innate difficulties that can be challenging to account for in the data analysis described in this paper. First, it is important to maintain a consistent camera position with respect to the object of interest to ensure that direct similarity shape analysis is appropriate. Otherwise, it may be more appropriate to consider projective shape analysis instead.

Finally, planar contours may commonly depict images of 3D objects. In the case that the object is relatively flat, such as with the stingrays in the example here, a slight shift in the camera angle may not result in a substantial change in the contour obtained from the digital image. However, for other 3D objects, such as the dogs and hand gestures, a slight shift may result in a drastic change in the form of the associated contour, which is an issue that has largely been ignored in the literature. In such cases, neither planar direct similarity shape nor planar projective shape may be an adequate descriptor for analyzing the contour data. Because of these issues, it is important to take great care with planar shape analysis of contours that arise from images of 3D solid objects. In such cases, where there is an absence of additional information on the scenes pictured, this care can help to ensure that a meaningful analysis can be conducted.

Acknowledgement

We are grateful to the organizers of the Analysis of Object Data program 2010/2011 at SAMSI, and, in particular, to Hans Georg Müller and to James O. Ramsey for useful conversations on infinite object data analysis regarded as data analysis on Hilbert manifolds. Thanks also to Rabi N. Bhattacharya and John T. Kent for discussions on the subject and to Ben Kimia and Shantanu H. Joshi for providing access to the silhouette data library.

References

- [1] Amaral, G. J. A. ; Dryden, I. L.; Patrangenaru, V. and Wood, A.T.A. (2010). Bootstrap confidence regions for the planar mean shape. *Journal of Statistical*

Planning and Inference. **140**, 3026-3034.

- [2] Azencott, R. (1994). Deterministic and random deformations ; applications to shape recognition. *Conference at HSSS workshop in Cortona, Italy*.
- [3] Azencott, R.; Coldefy, F. and Younes, L. (1996). A distance for elastic matching in object recognition Proceedings of 12th ICPR (1996), 687–691.
- [4] Bandulasiri, A.; Bhattacharya, R.N. and Patrangenaru, V. (2009) Nonparametric Inference for Extrinsic Means on Size-and-(Reflection)-Shape Manifolds with Applications in Medical Imaging. *Journal of Multivariate Analysis*. **100** 1867-1882.
- [5] Bandulasiri A. and Patrangenaru, V. (2005). Algorithms for Nonparametric Inference on Shape Manifolds, *Proc. of JSM 2005*, Minneapolis, MN, 1617-1622.
- [6] Bhattacharya A. and Bhattacharya, R. N. (2008). Statistics on Riemannian Manifolds: Asymptotic Distribution and Curvature. *Proceedings of the American Mathematical Society* 136. 2957-2967.
- [7] Bhattacharya, R.N; Ellingson, L; Liu, X; Patrangenaru, V; and Crane, M. (2012) Extrinsic Analysis on Manifolds is Computationally Faster than Intrinsic Analysis, with Application to Quality Control by Machine Vision. To appear in *Applied Stochastic Models in Business and Industry*.
- [8] Bhattacharya, R.N. and Patrangenaru, V. (2003). Large sample theory of intrinsic and extrinsic sample means on manifolds-Part I, *Ann. Statist.* **31**, no. 1, 1-29.
- [9] Bhattacharya, R.N. and Patrangenaru, V. (2005). Large sample theory of intrinsic and extrinsic sample means on manifolds- Part II, *Ann. Statist.*, **33**, No. 3, 1211-1245.
- [10] Dauxois, J., Pousse, A. and Romain, Y. (1982). Asymptotic theory for the principal component analysis of a vector random function: some applications to statistical inference. *J. Multivariate Anal.* **12**, 136–154.
- [11] Efron, B. (1979) Bootstrap methods: another look at the jackknife. *Ann. Statist.* **7**, No. 1, 1–26.
- [12] Fréchet, M. (1948). Les éléments aléatoires de nature quelconque dans un espace distancié. *Ann. Inst. H. Poincaré* **10**, 215–310.
- [13] Gaines, G. (2012). Random perturbation of a self-adjoint operator with a multiple eigenvalue. Dissertation. Department of Mathematics and Statistics, Texas Tech University.
- [14] Grenander, U. (1993). *General Pattern Theory*. Oxford Univ. Press.
- [15] Goodman, N. R. (1963). Statistical analysis based on a certain multivariate complex Gaussian distribution. (An introduction) *Ann. Math. Statist.* **34**, 152–177.

- [16] Hall, P. (1992). *The bootstrap and Edgeworth expansion*. Springer Series in Statistics, New York.
- [17] Hall, P., Müller, H.-G., Wang, J.-L. (2006). Properties of principal component methods for functional and longitudinal data analysis. *Ann. Statist.* **34**, 1493–1517.
- [18] Huckemann, S. and Ziezold, H. (2006). Principal component analysis for Riemannian manifolds, with an application to triangular shape spaces. *Adv. in Appl. Probab.* **38**, no. 2, 299–319.
- [19] Huckemann, S. and Hotz, T. (2009). Principal component geodesics for planar shape spaces. *J. Multivariate Anal.* **100**, no. 4, 699–714.
- [20] Joshi S.; Srivastava, A. ; Klassen, E. and Jermyn, I. (2007). Removing Shape-Preserving Transformations in Square-Root Elastic (SRE) Framework for Shape Analysis of Curves. *Workshop on Energy Minimization Methods in CVPR (EMM-CVPR)*. August.
- [21] Kaziska, D. and Srivastava, A. (2007). Gait-Based Human Recognition by Classification of Cyclostationary Processes on Nonlinear Shape Manifolds, *JASA*, 102(480): 1114-1124.
- [22] Kendall, D.G.; Barden, D.; Carne, T.K. and Le, H. (1999). *Shape and Shape Theory*. Wiley, New York.
- [23] Kendall, D.G. (1984), Shape manifolds, Procrustean metrics, and complex projective spaces. *Bull. London Math. Soc.* **16** 81-121.
- [24] Kent, J.T. (1992), New directions in shape analysis. *The Art of Statistical Science, A Tribute to G.S. Watson*, 115–127. Wiley Ser. Probab. Math. Statist. Probab. Math. Statist., Wiley, Chichester, 1992.
- [25] Kimia, Ben. A Large Binary Image Database. <http://www.lems.brown.edu/~dmc/>
- [26] Klassen, E.; Srivastava, A. ; Mio, W. and Joshi, S. H. (2004). Analysis of Planar Shapes Using Geodesic Paths on Shape Spaces, *IEEE Transactions on Pattern Analysis and Machine Intelligence* **26** 372 - 383.
- [27] Kume, A. and Le, H. (2003). On Fréchet means in simplex shape spaces. *Adv. in Appl. Probab.* **35** , 885–897.
- [28] Kume, A. and Le, H. (2000). Estimating Fréchet means in Bookstein’s shape space. *Adv. in Appl. Probab.* **32** , 663–674.
- [29] Lang, S. (1986) *Differential manifolds*. Springer, New York.
- [30] Le, H. (2001). Locating Fréchet Means with Application to Shape Spaces . *Advances in Applied Probability*, **33**. 324–338.

- [31] Le, H. and Kume, A. (2000). The Fréchet Mean Shape and the Shape of the Means. *Advances in Applied Probability*, **32**. 101-113
- [32] Le, H. and Kume, A.(2000). The Fréchet mean shape and the shape of the means. *Adv. in Appl. Probab.* **32** , 101–113.
- [33] Loève, M. (1977). *Probability Theory*(fourth ed.) Springer-Verlag, Berlin.
- [34] Michor, P. W. and Mumford, D. (2004). Riemannian Geometries on Spaces of Plane Curves. *Journal of the European Mathematical Society*, **8**, 1 - 48.
- [35] Mardia, K.V. and Patrangenaru, V. (2001) On affine and projective shape data analysis. In “Functional and Spatial Data Analysis”. *Proceedings of the 20th LASR Workshop, edited by K.V. Mardia& R.G. Aykroyd* , Leeds University Press, Leeds, 39–45.
- [36] Mio, W. and Srivastava, A. (2004). Elastic-String Models for Representation and Analysis of Planar Shapes. *Proceedings of the IEEE Computer Society International Conference on CVPR*.10–15.
- [37] Mio, W.; Srivastava, A. and Klassen, E. (2004)Interpolation by Elastica in Euclidean Spaces.*Quarterly ofApplied Math.* **62**, 359 - 378 .
- [38] Mio, W.; Srivastava, A. and Joshi, S. (2007). On the Shape of Plane Elastic Curves. *International Journal of Computer Vision*, **73**, 307–324.
- [39] Müller, H.-G., Stadtmüller, U. and Yao, F. (2006). Functional variance processes. *J. Amer. Statist. Assoc.* **101** 1007–1018.
- [40] Munk, A. and Dette, H. (1998) Nonparametric comparison of several regression functions: exact and asymptotic theory. *Ann. Statist.* **26**, 2339-2368.
- [41] Munk, A.; Paige, R.; Pang, J. ; Patrangenaru, V. and Ruymgaart, F. H.(2008). The One and Multisample Problem for Functional Data with Applications to Projective Shape Analysis. *J. of Multivariate Anal.* . **99**, 815-833.
- [42] Patrangenaru, V. (1998). Asymptotic Statistics on Manifolds, PhD Dissertation *Indiana University*.
- [43] Patrangenaru, V., Liu, X. and Sugathadasa, S. (2010). Nonparametric 3D Projective Shape Estimation from Pairs of 2D Images - I, In Memory of W.P. Dayawansa. *Journal of Multivariate Analysis.* **101**, 11-31.
- [44] Ramsay J. O. and Silverman, B. W. (2005). *Functional Data Analysis*, Springer Series in Statistics, Springer, 2nd edition.
- [45] Sebastian, T.B. ; Klein, P.N. and Kimia,B.B. (2003). On Aligning Curves. *IEEE Trans. Pattern Analysis and Machine Intelligence* **25**, no. 1, 116–125.
- [46] Small, C. G. (1996). *The Statistical Theory of Shape*, Springer-Verlag, New York.

- [47] Srivastava, A. and Klassen, P.E. (2002). Monte Carlo extrinsic estimators for manifold-valued parameters *IEEE Transactions on Signal Processing*, **50**, 299-308.
- [48] Srivastava, A. ; Joshi, S. Mio, W. and Liu, X. (2005). Statistical Shape Analysis: Clustering, Learning and Testing. *IEEE Trans. Pattern Analysis and Machine Intelligence*, **27**. 590–602.
- [49] Younes, L. (1998). Computable elastic distance between shapes. *SIAM Journal of Applied Mathematics*, **58**, 565-586.
- [50] Younes, L. (1999). Optimal matching between shapes via elastic deformations. *Journal of Image and Vision Computing*, **17**, 381-389.
- [51] Younes, L.; Michor, P. W.; Shah, J. and Mumford, D. (2008). A metric on shape space with explicit geodesics. *Rend. Lincei Mat. Appl.* **19** 25-57.
- [52] Zahn, C. T. and Roskies. (1972). Fourier Descriptors for Plane Closed Curves. *IEEE Tras. Computers* **21** 269-281.
- [53] Ziezold, H. (1998). Some aspects of random shapes. (English summary). *Numbers, information and complexity* (Bielefeld, 1998), 517–523, Kluwer Acad. Publ., Boston, MA.
- [54] Ziezold, H. (1994). Mean figures and mean shapes applied to biological figure and shape distributions in the plane. *Biometrical J.* **36**, no. 4, 491–510.
- [55] Ziezold, H. (1977). On expected figures and a strong law of large numbers for random elements in quasi-metric spaces. *Transactions of the Seventh Prague Conference on Information Theory, Statistical Decision Functions, Random Processes and of the Eighth European Meeting of Statisticians*, Vol. **A**, 591-602. Reidel, Dordrecht.